A Motion Control of a Two-Wheeled Mobile Robot

Kazuo Tsuchiya Takateru Urakubo Katsuyoshi Tsujita
Dept. of Aeronautics and Astronautics, Graduate School of Engineering, Kyoto University
Yoshida-Honmachi, Sakyo-ku, Kyoto City, Kyoto, 606-8501, Japan
urakubo@space.kuaero.kyoto-u.ac.jp

ABSTRACT

In this paper, we discuss a motion control of a two-wheeled mobile robot. In the design of a controller for the system, a kinematic model is usually used; The wheels don't skid at all and the mobile robot is regarded as a 3-dimensional 2-input nonholonomic system without drift. Many controllers based on the kinematic model have been proposed. However, in a real world, the wheels may skid on the ground or float away from the ground according to the rolling motion of the body. Therefore, we derive a dynamic model of a two-wheeled mobile robot which implies the translational motion with 3 degrees of freedom and the rotational motion with 3 degrees of freedom of the body and the rotational motion with one degree of freedom of each wheel, and then reduce the dynamic model to the kinematic model under certain assumptions. We design a controller based on the kinematic model by extending the Lyapunov control and analyze whether the designed controller works well in a real world by numerical simulations based on the dynamic model.

1. INTRODUCTION

One of the basic functions of robot is mobility, and mobile robots have mechanisms to realize the mobility such as legs or wheels. For this kind of robots, usually, the motion is determined by the kinematic relationship between the degrees of freedom of motion of the mechanism; For a wheeled robot, when the wheels don't skid, the motion is determined by the rotations of the wheels. This kind of dynamic system is called a nonholonomic system. A mobile robot is a nonholonomic system. For a nonholonomic system, the controller can be designed with the kinematic relationship as the state equation. From the viewpoint of control, a nonholonomic system has a difficult property; it is uncontrollable locally even if it is controllable globally. An effective and general algorithm to design a controller of a nonholonomic system has not been proposed yet. To control the motion of a mobile robot, a general method to design a controller of a nonholonomic system must be developed.

The controllers which have been proposed so far are classified as time-varying controllers and discontinuous time-invariant controllers. Time-varying controllers was originated by Samson ([3]). Sordalen and Egeland ([5]), and M'Closkey and Murray ([8]) proposed nonsmooth time-varying controllers which provide exponential rates of convergence.

On the other hand, discontinuous time-invariant feedback controllers have been proposed by Khennouf and Canudas de Wit ([2]). Astolfi proposed a method of designing a controller by transforming an original system through a nonsmooth coordinate transformation and designing a smooth time-invariant controller for the transformed system ([6], [7]). The controllers provide exponential rates of convergence.

The Lyapunov control is one of the design methods of a feedback controller of nonlinear systems; By setting a positive-definite function (Lyapunov function) which is minimized at the desired point and multiplying the gradient vector of the function by a symmetric positive-definite tensor, the control input is designed. When the Lyapunov control is applied to a nonholonomic system, the controlled system has equilibrium points besides the desired point and may stop at these points. We have proposed a design method by extending the Lyapunov method as follows ([15],[16]); First, we define a positive-definite function (Lyapunov function) which is minimized at the desired point. Then, we construct a tensor by superposing an asymmetric tensor on a symmetric positive-definite tensor and design the control input by multiplying the gradient vector of Lyapunov function by the tensor. When an extended Lyapunov control is applied to a nonholonomic system, the controlled system doesn't have an equilibrium point except the desired point and converges to the desired point. The designed controller is a discontinuous time-invariant feedback controller.

On the other hand, the development of the mobile robot which can carry out a task in a real world is desired now. So far, some experiments have been performed to check the robustness of the controller ([10]~[12]). Astolfi has performed an experiment for a two-wheeled mobile robot with a discontinuous controller ([7]). M'Closkey and Murray have performed an experiment for a mobile robot towing a trailer with a time-varying controller ([9]). In these experiments, the robustness for measurement noise or model errors in the kinematic model is checked under the assumption. There have been few researches which take account of the skid and the float of the wheels to check the validity of the kinematic model. A mobile robot doesn't always satisfy the kinematic relationship; the wheels often skid on the ground or float away from the ground according to the rolling motion of the body. When the motion controller of the mobile robot is designed based on the control theory for nonholonomic systems, it is important to examine the dynamic effect of the motion, the skid and the float of the wheels. For that purpose, a dynamic model of the mobile robot must be derived and the dynamic characteristics must be checked based on the model.

In this paper a motion control of a two-wheeled mobile robot is discussed. We derive a dynamic model of a two-wheeled mobile robot. This model implies the translational motion with 3 degrees of freedom and the rotational motion with 3 degrees of freedom of the body, and also implies the effect of the skid of the wheels. Then, we analyze the behavior of the two-wheeled mobile robot which is controlled by an extended Lyapunov control by numerical simulations based on the derived model. As a result, at the neighborhood of the point where the two-wheeled mobile robot performs a switch-back, the skid or the float of the wheels may be brought about according to the dynamics. But the frequency of the skid or the float becomes less as the two-wheeled mobile robot converges to the desired point. Finally, the two-wheeled mobile robot reaches the desired point.

2. A DYNAMIC MODEL OF A TWO-WHEELED MOBILE ROBOT

We consider a symmetrical two-wheeled mobile robot composed of three rigid links, the body and two wheels, as

0-7803-5731-0/99$10.00 ©1999 IEEE

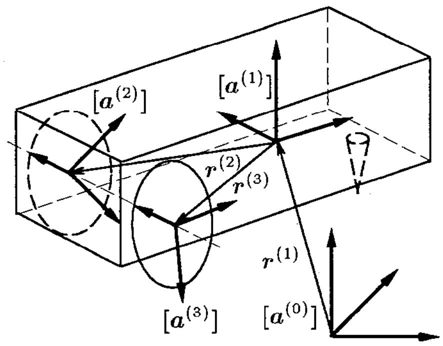

Figure 1: Schematic model of a two-wheeled mobile robot

shown in Fig.1. We assume that a rigid bar is attached on the front of the body so that the body is kept horizontal on the ground and that the rigid bar slips smoothly on the ground. Each wheel is driven by its own motor torque and touches the ground with a point. Frictional force acts on the points of the wheels. We derive an equation of motion of the two-wheeled mobile robot. The model implies the translational motion with 3 degrees of freedom and the rotational motion with 3 degrees of freedom of the body and the rotational motion with one degree of freedom of each wheel.

The body, the left wheel and the right wheel are labeled as link 1, 2 and 3. We introduce a set of unit vectors $\{a^{(0)}\} = \{a_1^{(0)} a_2^{(0)} a_3^{(0)}\}$ fixed in an inertia space and a set of unit vectors $\{a^{(i)}\} = \{a_1^{(i)} a_2^{(i)} a_3^{(i)}\}$ fixed in link i. The origin of $\{a^{(1)}\}$ is the total mass center of the three links and the origin of $\{a^{(i)}\}$ is the mass center of the link i $(i = 2,3)$. The direction of $a_1^{(1)}$ is toward the front of the body and the direction of $a_3^{(1)}$ is toward the top of the body. The direction of $a_2^{(i)}$ $(i = 1,2,3)$ coincides with the direction of the rotation axis of the wheels. Using these sets of unit vectors, we define the following column matrices;

$$\begin{aligned} [a^{(0)}]^T &= [a_1^{(0)} a_2^{(0)} a_3^{(0)}] \\ [a^{(1)}]^T &= [a_1^{(1)} a_2^{(1)} a_3^{(1)}] \\ [a^{(i)}]^T &= [a_1^{(i)}\, a_2^{(i)}\, a_3^{(i)}] \end{aligned}$$

We introduce the following vectors;

$\omega^{(k,l)}$: angular velocity of $\{a^{(k)}\}$ with respect to $\{a^{(l)}\}$
$\omega^{(k,l)} = [a^{(k)}]^T\, \omega^{(k,l)}$

$r^{(1)}$: position vector from the origin of $\{a^{(0)}\}$ to the origin of $\{a^{(1)}\}$
$r^{(1)} = [a^{(0)}]^T r^{(1)}$

$r^{(i)}$: position vector from the origin of $\{a^{(1)}\}$ to the origin of $\{a^{(i)}\}$ $(i = 2,3)$
$r^{(i)} = [a^{(1)}]^T r^{(i)}$

We define the following coordinate transform matrices;

$A^{(k,l)}$: a coordinate transform matrix from $\{a^{(k)}\}$ to $\{a^{(l)}\}$

We express the orientation of $\{a^{(1)}\}$ with respect to $\{a^{(0)}\}$ as Euler angles $\theta^{(1)}$ and the orientation of $\{a^{(i)}\}$ with respect to $\{a^{(1)}\}$ as Euler angles $\theta^{(i)}$ $(i = 2,3)$. We introduce the state variables as follows;

$$x^T = [\, \dot{r}^{(1)T}\ \omega^{(1,0)T}\ \omega^{(2,1)T}\ \omega^{(3,1)T}]\, . \tag{1}$$

When the variable,

$$\theta^T = [\, r^{(1)T}\ \theta^{(1)T}\ \theta^{(2)T}\ \theta^{(3)T}]\, , \tag{2}$$

is introduced, we obtain

$$x = S\dot{\theta}\, , \tag{3}$$

where

$$S = \begin{bmatrix} I & \mathbf{0} & \mathbf{0} & \mathbf{0} \\ \mathbf{0} & S_3(\theta_2^{(1)})S_2(\theta_3^{(1)}) & \mathbf{0} & \mathbf{0} \\ \mathbf{0} & \mathbf{0} & I & \mathbf{0} \\ \mathbf{0} & \mathbf{0} & \mathbf{0} & I \end{bmatrix} .$$

$$S_2(\theta) = \begin{bmatrix} \cos\theta & 0 & 0 \\ 0 & 1 & 0 \\ \sin\theta & 0 & 1 \end{bmatrix}$$

$$S_3(\theta) = \begin{bmatrix} \cos\theta & \sin\theta & 0 \\ -\sin\theta & \cos\theta & 0 \\ 0 & 0 & 1 \end{bmatrix}$$

I : 3×3 unit matrix
$\mathbf{0}$: 3×3 zero matrix

The kinetic energy T of the total system is expressed as

$$2T = x^T H^T (\hat{\mathcal{L}}^T M \hat{\mathcal{L}} + J) H x\, , \tag{4}$$

where

$$\hat{\mathcal{L}} = \begin{bmatrix} \mathbf{0} & \mathbf{0} & \mathbf{0} & \mathbf{0} \\ A^{(1,0)} & \mathbf{0} & \mathbf{0} & \mathbf{0} \\ A^{(2,0)} & A^{(2,1)}\tilde{r}^{(2)} & \mathbf{0} & \mathbf{0} \\ A^{(3,0)} & A^{(3,1)}\tilde{r}^{(3)} & \mathbf{0} & \mathbf{0} \end{bmatrix} , \tag{5}$$

$$H = \begin{bmatrix} I & \mathbf{0} & \mathbf{0} & \mathbf{0} \\ \mathbf{0} & I & \mathbf{0} & \mathbf{0} \\ \mathbf{0} & A^{(2,1)} & I & \mathbf{0} \\ \mathbf{0} & A^{(3,1)} & \mathbf{0} & I \end{bmatrix} , \tag{6}$$

$$M = \begin{bmatrix} \mathbf{0} & \mathbf{0} & \mathbf{0} & \mathbf{0} \\ \mathbf{0} & m^{(1)}I & \mathbf{0} & \mathbf{0} \\ \mathbf{0} & \mathbf{0} & m^{(2)}I & \mathbf{0} \\ \mathbf{0} & \mathbf{0} & \mathbf{0} & m^{(3)}I \end{bmatrix} , \tag{7}$$

$$J = \begin{bmatrix} \mathbf{0} & \mathbf{0} & \mathbf{0} & \mathbf{0} \\ \mathbf{0} & J^{(1)} & \mathbf{0} & \mathbf{0} \\ \mathbf{0} & \mathbf{0} & J^{(2)} & \mathbf{0} \\ \mathbf{0} & \mathbf{0} & \mathbf{0} & J^{(3)} \end{bmatrix} , \tag{8}$$

and we use the following quantities;

$m^{(1)}$: mass of the body
$m^{(i)}$: mass of the wheel i , $m^{(2)} = m^{(3)}$
$J^{(1)}$: inertia matrix of the body about the origin of $\{a^{(1)}\}$
$J^{(i)}$: inertia matrix of the wheel i about the origin of $\{a^{(i)}\}$

We define a matrix $\tilde{h}$ corresponding to a vector $h^T = [\, h_1\, , h_2\, , h_3\,]$ as follows,

$$\tilde{h} = \begin{bmatrix} 0 & h_3 & -h_2 \\ -h_3 & 0 & h_1 \\ h_2 & -h_1 & 0 \end{bmatrix} .$$

The generalized momentum $\hat{L}$ for the state variable x is computed as

$$\begin{aligned} \hat{L} &= \begin{bmatrix} \hat{L}^{(0)} \\ \hat{L}^{(1)} \\ \hat{L}^{(2)} \\ \hat{L}^{(3)} \end{bmatrix} = \left(\frac{\partial T}{\partial x}\right)^T + \left(\frac{\partial T}{\partial x^T}\right) \\ &= H^T (\hat{\mathcal{L}}^T M \hat{\mathcal{L}} + J) H x\, . \end{aligned} \tag{9}$$

The components of $\hat{L}$ are physically interpreted as

$[\boldsymbol{a}^{(0)}]^T\hat{L}^{(0)}$: translation momentum of the total system

$[\boldsymbol{a}^{(1)}]^T\hat{L}^{(1)}$: angular momentum of the total system about the origin of $\{\boldsymbol{a}^{(1)}\}$

$[\boldsymbol{a}^{(i)}]^T\hat{L}^{(i)}$: angular momentum of the wheel i about the origin of $\{\boldsymbol{a}^{(i)}\}$

Using $\hat{L}$, the equation of motion is derived as follows,

$$\dot{\hat{L}} + \Omega\hat{L} = \hat{G}\ , \tag{10}$$

where

$$\Omega = \begin{bmatrix} \mathbf{0} & \mathbf{0} & \mathbf{0} & \mathbf{0} \\ \mathbf{0} & \tilde{\omega}^{(1,0)T} & \mathbf{0} & \mathbf{0} \\ \mathbf{0} & \mathbf{0} & \tilde{\omega}^{(2,0)T} & \mathbf{0} \\ \mathbf{0} & \mathbf{0} & \mathbf{0} & \tilde{\omega}^{(3,0)T} \end{bmatrix}, \tag{11}$$

and $\hat{G}$ is a generalized force computed as follows,

$$\hat{G}^T = \left[\hat{G}^{(0)T}\ 0\ 0\ 0\ \hat{G}^{(2)T}\ \hat{G}^{(3)T}\right]\ , \tag{12}$$

$$\hat{G}^{(0)T} = (m^{(1)} + m^{(2)} + m^{(3)})[0, 0, g_0]\ ,$$

$$\hat{G}^{(i)T} = [\tau_1^{(i)}, \tau_2^{(i)}, \tau_3^{(i)}]\ ,$$

where g_0 is the gravity acting on the unit mass and $\tau_2^{(i)}$ is torque to drive the wheel i.

Two types of kinematic constraints for the system are considered. One is the constraint that, when a wheel or the bar on the body doesn't float away from the ground, the height of the point touching the ground is constant. We express this type of constraints as $\Phi = 0$. The other is the constraint that, when a wheel doesn't skid on the ground, the velocity of the point of the wheel touching the ground is zero in a horizontal plane. We express this type of constraints as $\Psi = 0$.

$$\Phi = \begin{bmatrix} \Phi_3^{(1)}(\theta) \\ \Phi_3^{(2)}(\theta) \\ \Phi_3^{(3)}(\theta) \end{bmatrix} = 0\ ,\ \Psi = \begin{bmatrix} \Psi_1^{(2)}(\theta, z) \\ \Psi_2^{(2)}(\theta, z) \\ \Psi_1^{(3)}(\theta, z) \\ \Psi_2^{(3)}(\theta, z) \end{bmatrix} = 0\ . \tag{13}$$

If some of the constraints are satisfied, the constraints and the equation of motion, Eq.(10), are put together by the method of Lagrange undetermined multiplier;

$$\dot{\hat{L}} + \Omega\hat{L} = \hat{G} + (E^T S^{-1})^T \Gamma_{\Phi} + K\Lambda_{\Psi}\ , \tag{14}$$

where

$$E^T = \frac{\partial\Phi}{\partial\theta}\ ,\ K^T = \frac{\partial\Psi}{\partial z}\ , \tag{15}$$

and Γ_{Φ}, Λ_{Ψ} are Lagrange undetermined multipliers. The motion of the two-wheeled mobile robot is determined by the equation of motion, Eq.(14), and the constraints, Eq.(13).

3. DESIGN OF A CONTROLLER

Basic Equation for Design of a Controller

We assume that the wheels or the bar doesn't float away from the ground and that the wheels of the two-wheeled mobile robot don't skid at all. Then, translational velocity u_1 and angular velocity u_2 of the mobile robot are determined by the following kinematic relationship;

$$\begin{bmatrix} u_1 \\ u_2 \end{bmatrix} = \begin{bmatrix} D/2 & D/2 \\ -D/R & D/R \end{bmatrix} \begin{bmatrix} \dot{\theta}_2^{(2)} \\ \dot{\theta}_2^{(3)} \end{bmatrix}\ , \tag{16}$$

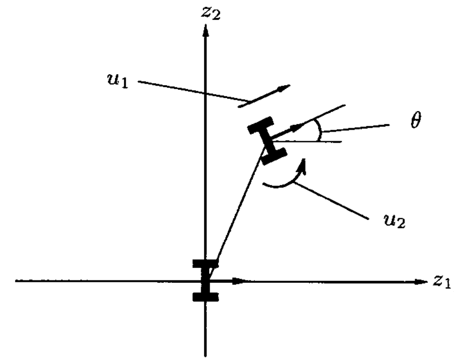

Figure 2: State variables, z_1, z_2 and θ, and inputs, u_1 and u_2, of a two-wheeled mobile robot

where D is the radius of each wheel and R is the distance between the two wheels. We consider the following feedback law of the torque $\tau_2^{(i)}$ to the wheel i;

$$\begin{bmatrix} \tau_2^{(2)} \\ \tau_2^{(3)} \end{bmatrix} = -K_t\left(\begin{bmatrix} \dot{\theta}_2^{(2)} \\ \dot{\theta}_2^{(3)} \end{bmatrix} - \begin{bmatrix} D/2 & D/2 \\ -D/R & D/R \end{bmatrix}^{-1} \begin{bmatrix} \hat{u}_1 \\ \hat{u}_2 \end{bmatrix}\right), \tag{17}$$

where K_t is a constant, and $\hat{u}_1$ and $\hat{u}_2$ are given reference velocities. When the feedback gain K_t is large, translational velocity u_1 and angular velocity u_2 of the mobile robot follow the reference velocities fast. Then, we assume that translational velocity u_1 and angular velocity u_2 of the mobile robot can be arbitrarily controlled and regarded as the inputs of the system. Under this assumption, the motion of the two-wheeled mobile robot is determined by the following equation derived from Eq.(13) and Eq.(14),

$$\frac{d\boldsymbol{z}}{dt} = B\boldsymbol{u}\ , \tag{18}$$

$$\boldsymbol{z} = \begin{bmatrix} z_1 \\ z_2 \\ \theta \end{bmatrix}\ ,\ B = \begin{bmatrix} \cos\theta & 0 \\ \sin\theta & 0 \\ 0 & 1 \end{bmatrix}\ ,\ \boldsymbol{u} = \begin{bmatrix} u_1 \\ u_2 \end{bmatrix}\ ,$$

where, as shown in Fig.2, the state of the two-wheeled mobile robot is expressed in terms of the position of the mobile robot on the plane, z_1 and z_2, and the angle θ between the current direction of the mobile robot and the positive direction of the z_1 axis. The desired point is set to be the origin. It is well known that this system is controllable at all points ([15]).

A Controller Based on the Extended Lyapunov Control

We have proposed a method to design a controller for a 3-dimensional 2-input nonholonomic system without drift based on the extended Lyapunov control ([15],[16]). We introduce the following Lyapunov function;

$$V(\boldsymbol{z}) = \frac{1}{2}(m_1 z_1^2 + m_2 z_2^2 + m_3 z_3^2)\ , \tag{19}$$

where m_1, m_2 and m_3 are positive constants. The input vector is designed as follows;

$$\boldsymbol{u} = \alpha(\boldsymbol{u}_s + \beta\boldsymbol{u}_a)\ , \tag{20}$$

where α and β are positive constants,

$$\boldsymbol{u}_s = -I_s B^T \nabla V\ , \tag{21}$$

$$\boldsymbol{u}_a = -\frac{z_2}{h(g)} I_a B^T \nabla V\ , \tag{22}$$

$$I_s = \begin{bmatrix} 1 & 0 \\ 0 & 1 \end{bmatrix} , \quad I_a = \begin{bmatrix} 0 & 1 \\ -1 & 0 \end{bmatrix} ,$$

$$g = |B^T \nabla V| = \sqrt{(z_1 \cos\theta + z_2 \sin\theta)^2 + \theta^2} , \quad (23)$$

$$\nabla = \left[\frac{\partial}{\partial z_1}, \frac{\partial}{\partial z_2}, \frac{\partial}{\partial \theta} \right]^T ,$$

and $h(g)$ is a smooth function such that

$$h(0) = 0 \ , \quad h(g) > 0 \text{ for } g > 0 . \quad (24)$$

We define

$$\frac{1}{h(g)} B^T \nabla V = 0 \ \text{ at } B^T \nabla V = 0 . \quad (25)$$

The term $\boldsymbol{u}_s$ in the input $\boldsymbol{u}$, Eq.(21), moves the system so that the value of the Lyapunov function V decreases. Since the term $\boldsymbol{u}_s$ is zero on the line, $g = 0$, the system stops at a point on the line if the input $\boldsymbol{u}$ consists of only the term $\boldsymbol{u}_s$. While, the term $\boldsymbol{u}_a$ in the input $\boldsymbol{u}$, Eq.(22), moves the system so that the value of the Lyapunov function V is constant, and keeps the system away from the line, $g = 0$.

Taking account of the characteristics of $\boldsymbol{u}_s$ and $\boldsymbol{u}_a$, it is expected that the system with the input vector (20) moves away from the line, $g = 0$, reduces the value of the Lyapunov function $V(t)$, and converges to the origin as $V \to 0$. The derivative of the Lyapunov function becomes to be composed of a symmetric and an asymmetric bilinear form in the gradient vectors. We will call the control with this type of input as an extended Lyapunov control. It is noteworthy that the coefficient of the asymmetric matrix is determined by Lie bracket which indicates the controllability of the system.

4. THE BEHAVIOR OF THE CONTROLLED SYSTEM

Basic equation (18) with the input (20) becomes

$$\frac{dz}{dt} = -\alpha B(I_s + \beta \frac{z_2}{h(g)} I_a) B^T \nabla V . \quad (26)$$

Since the parameter α affects only the time scale, without loss of generality, the paremeter α can be set to be 1.0 ; for $t_1 = \alpha t$, $\frac{dz}{dt_1} = -B(I_s + \beta \frac{z_2}{h(g)} I_a) B^T \nabla V$. We have analyzed the behavior of the system (26) in [13], [14] and [16], setting the parameters of the Lyapunov function (19), m_1, m_2 and m_3, to be 1.0 , and the parameter α to be 1.0.

Dynamic Characteristics

With Eq.(26), the derivative of $V(t)$ is computed as

$$\begin{aligned} \dot{V} &= -(B^T \nabla V)^T (I_s + \beta \frac{z_2}{h(g)} I_a) B^T \nabla V \\ &= -|B^T \nabla V|^2 \leq 0 . \end{aligned} \quad (27)$$

The equilibrium points of the controlled system, Eq.(26), are the points on the line, $g = 0$. From Eq.(23), the line, $g = 0$, coincides with the z_2 axis. Equation (27) shows that the controlled system converges to the line. We will examine the stability of the points on the line. Since, on the line, the basic equation (26) is discontinuous, for the sake of analysis, we modify Eq.(26) as follows;

$$\dot{z} = -B(I_s + \beta \tanh\left(\frac{h(g)}{\epsilon}\right) \frac{z_2}{h(g)} I_a) B^T \nabla V. \quad (28)$$

Equation (28) becomes to be Eq.(26) as ϵ becomes to be zero. By linearizing Eq.(28) in the neighborhood of the equilibrium points, the stability of the system on the z_2 axis is revealed as follows;

$$\begin{cases} |z_2| < \sqrt{\frac{2\epsilon}{\beta}} & \Longleftrightarrow \quad \text{stable focus} \\ \sqrt{\frac{2\epsilon}{\beta}} < |z_2| < 2\sqrt{1+\frac{\epsilon}{\beta}} & \Longleftrightarrow \quad \text{unstable focus} \\ |z_2| > 2\sqrt{1+\frac{\epsilon}{\beta}} & \Longleftrightarrow \quad \text{unstable node} \end{cases} \quad (29)$$

As the result, as ϵ becomes to be zero, the origin becomes to be the only stable equilibrium point of the system (28). Therefore, the stable equilibrium point of the system (26) becomes to be only the origin.

We set the function $h(g)$ to be g or g^2, and analyze in detail the behavior of the system in the neighborhood of the origin.

(1) The function $h(g)$ is set to be

$$h(g) = g \ . \quad (30)$$

Then, the following approximate solutions of the variables z and g are obtained;

$$\begin{aligned} z_1 &= g\cos(\omega_{c1} t + \phi_1) , \\ \theta &= g\sin(\omega_{c1} t + \phi_1) , \end{aligned} \quad (31)$$

$$|z_2| = \frac{1}{\sqrt{\frac{\beta^2}{2} t + C}} , \quad (32)$$

$$g = \frac{\beta}{\beta^2 t + 2C} , \quad (33)$$

where C and ϕ_1 are constant, and $\omega_{c1} = \frac{\beta z_2}{g}$. Expression (31) shows that the amplitude of oscillation decreases as $O(t^{-1})$ while the frequency of oscillation increases as $O(t^{\frac{1}{2}})$. On the other hand, input u decreases as $O(t^{-\frac{1}{2}})$ and tends to zero as $t \to \infty$.

(2) The function $h(g)$ is set to be

$$h(g) = g^2 \ . \quad (34)$$

First, we consider the behavior of the system in the region where $g^2 < O(\beta|z_2|)$. In the region the following approximate solutions of the variables z and g are obtained;

$$\begin{aligned} z_1 &= g\cos(\omega_{c2} t + \phi_2) , \\ \theta &= g\sin(\omega_{c2} t + \phi_2) , \end{aligned} \quad (35)$$

$$z_2 = C_1 e^{-\frac{\beta}{2} t} , \quad (36)$$

$$\begin{cases} \beta \neq 2 \ : \ g = \sqrt{C_2 e^{-2t} + \frac{\beta}{2-\beta} C_1^2 e^{-\beta t}} \\ \beta = 2 \ : \ g = \sqrt{(\beta C_1^2 t + C_2) e^{-2t}} \end{cases} , \quad (37)$$

where C_1, C_2 and ϕ_2 are constant, and $\omega_{c2} = \frac{\beta z_2}{g^2}$.

When $\beta < 4.0$, the system satisfies that $g^2 < O(\beta|z_2|)$ for all $t > 0$. As the time goes on, the amplitude of oscillation of the inputs u_1 and u_2 becomes to be a constant, $\sqrt{\beta(2-\beta)}$, if $\beta < 2.0$ and becomes to be 0 if $2.0 \leq \beta < 4.0$. The frequency of oscillation of the inputs, as the time goes on, becomes to be large exponentially.

Table 1: Simulation cases (kinematic model)

	$h(g)$	α	β	Initial Value of z^T
Case (1-a)	g	-	1.0	(0.01 , 1.0 , 0.01)
Case (1-b)	g	-	10.0	(0.01 , 1.0 , 0.01)
Case (2-a)	g^2	-	1.0	(0.5 , 1.0 , 0.0)
Case (2-b)	g^2	-	5.0	(0.5 , 1.0 , 0.0)

When $\beta > 4.0$, the system can't satisfy that $g^2 < O(\beta|z_2|)$ for all $t > 0$ and, as the time goes on, goes toward the region where $g^2 \geq O(\beta|z_2|)$. As the time goes on, the amplitude and the frequency of oscillation of the inputs u_1 and u_2 become to be small exponentially, as long as the solutions, Eq.(36) and Eq.(37), are proper.

Next, we consider the behavior of the system in the region where $g^2 \geq O(\beta|z_2|)$. In the region we obtain the equation for g as

$$\dot{g} = -g \ . \tag{38}$$

If $g^2 \geq O(\beta|z_2|)$ for all $t > 0$, from Eq.(38), we obtain

$$g = C_3 e^{-t} \ , \tag{39}$$

where C_3 is constant. Then, since $|z_2| \leq O(e^{-2t})$, the system converges to the origin and the magnitude of the inputs converges to 0. According to the initial value of the system and the value of the parameter β, the system can't satisfy that $g^2 < O(\beta|z_2|)$ for all $t > 0$ and, as the time goes on, may go toward the region where $g^2 < O(\beta|z_2|)$. If the system moves into the region where $g^2 < O(\beta|z_2|)$, the system behaves as the above analysis.

As a result of these analyses, we obtain the following conclusion; The controlled system converges to the origin exponentially. The behavior of the system is different according to the value of the parameter β and initial conditions. The magnitude of the inputs becomes to be 0 or a constant, as the time goes on.

Numerical Examples

Numerical simulations were executed to check the analysis based on Eq.(18). First, the simulation results where $h(g) = g$ are shown.

Case (1-a) ; The value of the parameter β is set to be 1.0 and the system converges to the origin as shown in Fig.3. First, the system approaches the curved surface, $g = \frac{\beta}{2} z_2^2$, and then, converges to the origin, the desired point, along that curved surface. This result also consists with the solutions of the variables g and z_2, Eq.(33) and Eq.(32).

Case (1-b) ; The value of the parameter β is set to be 10.0 and good performance of control is realized. Figure 4 shows the motion of the system in z_1 and z_2 plane. In this case, first, the system moves to the neighborhood of the desired point after three large switch-backs. Then, in the neighborhood of the origin, the system behaves in the same way as in Case (1-a); the variables z_1 and θ oscillate with a high frequency. But, in practice, we may avoid this oscillation, if we cease control in a neighborhood of the desired point.

Next, the simulation results where $h(g) = g^2$ are shown.

Case (2-a) ; The value of the parameter β is set to be 1.0. The variables z_2 and g behave as the solutions, Eq.(36) and Eq.(37). Figure 5 shows the behavior of the system in z_1 and z_2 plane. The amplitude of oscillation of the inputs, u_1 and u_2, converges to a constant, 1.0, as shown in Fig.6.

Case (2-b) ; The value of the parameter β is set to be 5.0. Figure 7 shows the motion of the system in z_1 and z_2 plane. In this case, the system moves to the neighborhood of the desired point after two large switch-backs, and, in the neighborhood of the origin, converges to the origin exponentially without the oscillation of the variables z_1 and θ. The time history of variable g matches the solution, Eq.(39), very well. The inputs, u_1 and u_2, converge to zero and don't oscillate with a high frequency as shown in Fig.8.

From the above results, taking account of the rate of the convergence of the system and the oscillation and the magnitude of the inputs, the control performance in Case (2-b) is the best. Therefore, we recommend to set the function $h(g)$ to be g^2 and the parameter β to be larger than 4.0.

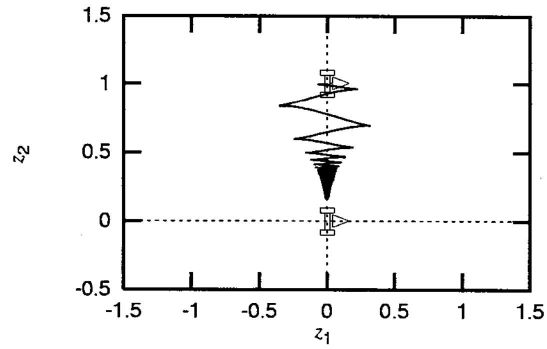

Figure 3: The motion of the system in z_1-z_2 plane (Case (1-a))

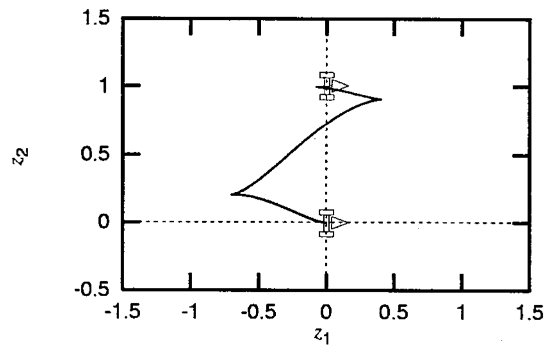

Figure 4: The motion of the system in z_1-z_2 plane (Case (1-b))

5. NUMERICAL SIMULATIONS BASED ON A DYNAMIC MODEL

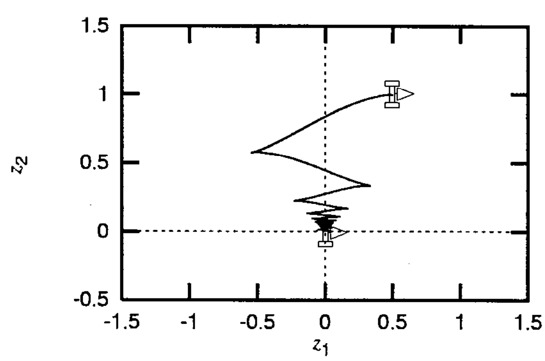

Figure 5: The motion of the system in z_1-z_2 plane (Case (2-a))

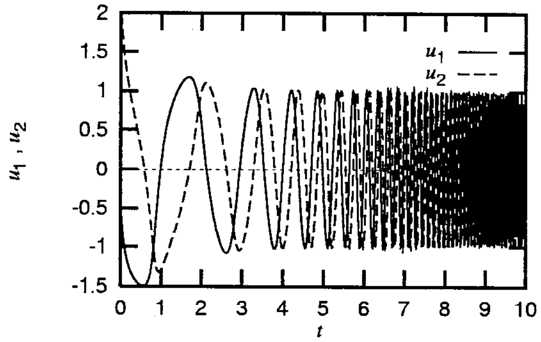

Figure 6: Time history of u_1, u_2 (Case (2-a))

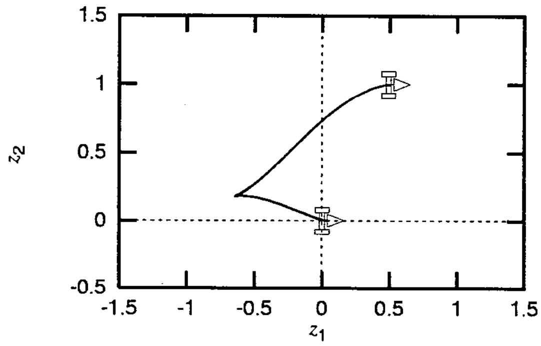

Figure 7: The motion of the system in z_1-z_2 plane (Case (2-b))

In Sec.3 we design a controller for a two-wheeled mobile robot under the condition that the wheels don't skid at all and that translational velocity u_1 and angular velocity u_2 are regarded as the inputs of the system. But in a real world the wheels may skid or float away from the ground and the inputs of the system are torques to the wheels. Therefore, in this section, we check whether the designed controller works well in a real world by numerical simulations based on the dynamic model derived in Sec.2. Values of parameters of two-wheeled mobile robot are given in Table 2.

In numerical simulations, we use the input torques to the wheels, Eq.(17), substituting the feedback law $\boldsymbol{u}(\boldsymbol{z})$, Eq.(20), into Eq.(17) as referenced velocities $\hat{u}_1$ and $\hat{u}_2$. We set the feedback gain K_t so that the frequency band width of the controller is to about 1.6 Hz. We assume that the following frictional force acts on the point of the wheel touching the ground; When a wheel doesn't skid, static friction acts on the point and the frictional force is up to the maximum static frictional force μF, where μ is a coefficient of static friction and F is the normal reaction force exerted to the point of the wheel. When a wheel is skidding, kinetic friction acts on the point and the frictional force $\boldsymbol{k}$ is expressed as

$$\boldsymbol{k} = -(\mu' \frac{1}{|\boldsymbol{v}_s|} + \nu) F \boldsymbol{v}_s \tag{40}$$

where μ' is a coefficient of kinetic friction, ν is a coefficient of viscous friction and $\boldsymbol{v}_s$ is the velocity vector of the point of the wheel touching the ground. The parameters, μ, μ' and ν, are set to be 0.8, 0.3 and 1.0[s/m] respectively.

We executed numerical simulations based on the dynamic model, Eq.(10), which correspond to Case (1-b) and (2-b) in the kinematic model that show a good control performance of the system. Initial values of the state variable

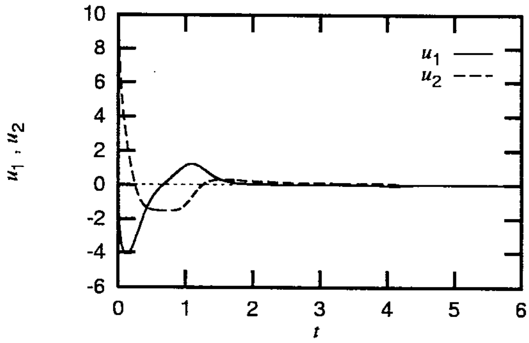

Figure 8: Time history of u_1, u_2 (Case (2-b))

Table 2: Values of system parameters

main body	length	100	[cm]
	width	80.0	[cm]
	height	80.0	[cm]
	mass	50.0	[kg]
wheel	diameter	50.0	[cm]
	mass	3.0	[kg]

$\boldsymbol{z}$, the parameters, α and β, in Eq.(20) and the function $h(g)$ are summarized as in Table 3. Case A, B and C are corresponding to Case (1-b), and Case D, E and F are corresponding to Case (2-b). As the parameter α becomes to be large, the referenced velocities, $\hat{u}_1$ and $\hat{u}_2$ become to be large and the dynamic effect of the motion of the system becomes to be crucial. The simulation results are shown in Fig.9 and 10. In Case A and D, the wheels don't skid at all and the trajectories of the system in z_1 and z_2 plane are similar to the ones in Case (1-b) and (2-b). Times taken for the system to reach the neighborhood of the desired point are about 500 [s] in Case A and about 100 [s] in Case D. In Case B and E, although the times become to be short according to the value of the parameter α, at least one of the two wheels is skidding on the dashed line. In Case C and F, since the skid of the wheels shown by dashed lines is intensive than Case B and E, the trajectories of the system are remarkably different from the ones in Case (1-b) and (2-b). Moreover, the bar attached on the body floats away from the ground on the dash-dotted line between the symbols + in Case C. However, in each case, the skid of the wheels fades out as the time goes on, and then the mobile robot goes toward the desired state. Times taken for the system to reach the neighborhood of the desired point are about 50 [s] in Case B , about 15 [s] in Case C, about 30 [s] in Case E and about 3 [s] in Case F.

From the above result, if the value of the parameter α is small, it is proper to design the controller based on the kinematic model. But, if the value of the parameter α becomes to be large, the motion of the system with the controller is remarkably different from the motion of the system based on the kinematic model because of the dynamic effect of the motion of the system. Nevertheless, after the skid of the wheels fades out, the system goes toward the desired state in the above numerical results. It is caused by the fact that the designed controller is a feedback controller.

6. CONCLUSIONS

In this paper, we designed a controller of a two-wheeled mobile robot and analyzed whether the designed controller works well in a real world by numerical simulations. In a real world, the wheels may skid on the ground or float

Table 3: Simulation cases (dynamic model)

	$h(g)$	α	β	Initial Value z^T
Case A	g	0.01	10.0	(0.01 , 1.0 , 0.01)
Case B	g	0.1	10.0	(0.01 , 1.0 , 0.01)
Case C	g	0.3	10.0	(0.01 , 1.0 , 0.01)
Case D	g^2	0.06	5.0	(0.5 , 1.0 , 0.0)
Case E	g^2	0.2	5.0	(0.5 , 1.0 , 0.0)
Case F	g^2	3.0	5.0	(0.5 , 1.0 , 0.0)

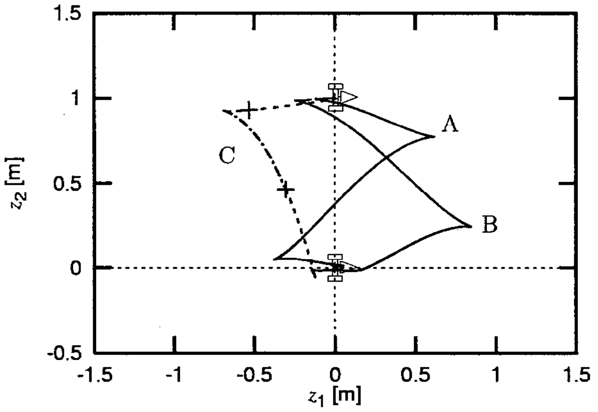

Figure 9: The motion of the system in z_1-z_2 plane (Case A, B and C)

away from the ground according to the rolling motion of the body. Therefore we derived a dynamic model of a two-wheeled mobile robot which implies the translational motion with 3 degrees of freedom and the rotational motion with 3 degrees of freedom of the body and the rotational motion with one degree of freedom of each wheel. The derived dynamic model is transformed to a kinematic model under the assumption that the wheels don't skid at all and translational velocity and rotational velocity of the body of the mobile robot are regarded as inputs of the system. We designed a controller for the kinematic model by extending the Lyapunov control and verified that the designed controller works well in a real world by numerical simulations based on the dynamic model.

7. REFERENCES

[1] R. W. Brockett : Asymptotic Stability and Feedback Stabilization, Differential Geometric Control Theory-Progress in Mathematics, **27**, 181/191, Springer-Verlag, 1983

[2] H. Khennouf and C. Canudas de Wit : Quasi-continuous Exponential Stabilizers for Nonholonomic Systems, International Federation of Automatic Control 13th World Congress, 2b-174, San Francisco, USA, 1996

[3] C. Samson : Control of Chained Systems Application to Path Following and Time-Varying Point-Stabilization of Mobile Robots, IEEE Trans. on Automatic Control, **40**-1, 64/77, 1995

[4] J.-B. Pomet : Explicit Design of Time-varying Stabilizing Control Laws for a Class of Controllable Systems without Drift, System & Control Letters, **18**, 147/158, 1992

[5] O. J. Sordalen and O. Egeland : Exponential Stabilization of Nonholonomic Chained Systems, IEEE Trans. on Automatic Control, **40**-1, 35/49, 1995

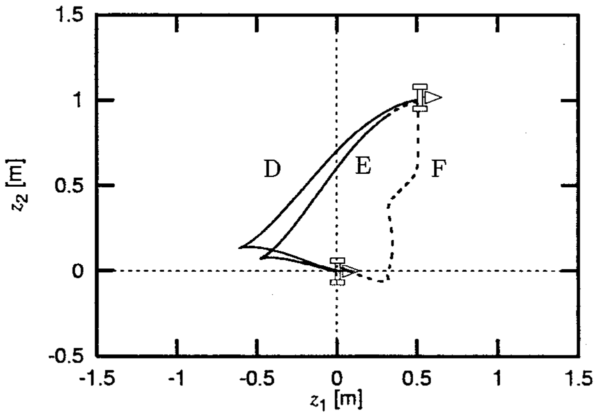

Figure 10: The motion of the system in z_1-z_2 plane (Case D, E and F)

[6] A. Astolfi : Discontinuous Control of Nonholonomic Systems, System & Control Letters, 1996

[7] A. Astolfi : Exponential Stabilization of a Wheeled Mobile Robot via Discontinuous Control, ASME, Journal of Dynamic Systems Measurement and Control, March, 1999

[8] R. T. M'Closkey and R. M. Murray : Exponential Stabilization of Driftless Nonlinear Control Systems Using Homogeneous Feedback, CDS Technical Report CDS 95-012

[9] R. T. M'Closkey and R. M. Murray : Experiments in Exponential Stabilization of a Mobile Robot towing a Trailer, American Control Conference, Baltimore, Maryland, 1994

[10] F. Bullo and R. M. Murray : Experimental Comparison of Trajectory Trackers for a Car with Trailers, IFAC World Congress, San Francisco, July, 1996

[11] S. Sekhavat, F. Lamiraux, J.P. Laumond, G. Bauzil and A. Ferrand : Motion Planning and Control for Hilare Pulling a Trailer: Experimental Issues, IEEE International Conference on Robotics and Automation, Albuquerque, USA, 1997

[12] K. Ishikawa, K. Fujimoto and T. Sugie : Feedback Control of Two-Wheeled Vehicle based on Generalized Canonical Transformation, Proc. 43rd Annual Conference of ISCIE, Japan, 1999

[13] K. Tsuchiya, T. Urakubo and K. Tsujita : A Feedback Control for a Class of Non-holonomic System, Proc. 7th Workshop on Astrodynamics and Flight Mechanics, ISAS, 56/61, 1997

[14] K. Tsuchiya, T. Urakubo and K. Tsujita : A Feedback Control of a Two Wheeled Vehicle, Proc. Conference on Robotics and Mechatronics, 2AIII2-5 , Sendai, Japan, 1998 (in Japanese)

[15] K. Tsuchiya, T. Urakubo and K. Tsujita : A Motion Control of a Space Manipulator by a Generalized Lyapunov Control, Proc. 8th Workshop on Astrodynamics and Flight Mechanics, ISAS, 36/41, 1998

[16] K. Tsuchiya, T. Urakubo and K. Tsujita : A Motion Control of a Non-holonomic System by an Extension of Lyapunov Control, submitted to Jornal of Guidance, Control, and Dynamics